

A GLIMPSE INTO THE PAST: THE RECENT EVOLUTION OF GLOBULAR CLUSTERS^{1,2}JASONJOT S. KALIRAI^{3,5}, JAY STRADER^{4,5}, JAY ANDERSON⁶, AND HARVEY B. RICHER⁷*Draft version February 10, 2022*

ABSTRACT

We present the serendipitous discovery of 195 extragalactic globular clusters (GCs) in one of the deepest optical images ever obtained, a 126 orbit *Hubble Space Telescope* (*HST*) Advanced Camera for Surveys (ACS) imaging study of the nearby Galactic GC NGC 6397. The distant GCs are all found surrounding a bright elliptical galaxy in the field, and are among the faintest objects detected in the image, with magnitudes $26 \lesssim F814W \lesssim 30$. We measure the redshift of the parent elliptical galaxy, using the Gemini Multi-Object Spectrograph (GMOS) on Gemini South, to be $z = 0.089$ (375 Mpc). This galaxy, and its associated clusters, therefore ranks as one of the most distant such systems discovered to date. The measured light from these clusters was emitted 1.2 Gyr ago (the lookback time) and therefore the optical properties hold clues for understanding the evolution of GCs over the past Gyr. We measure the color function of the bright GCs and find that both a blue and red population exist, and that the colors of each sub-population are redder than GCs in local elliptical galaxies of comparable luminosity. For the blue clusters, the observed color difference from $z = 0.089$ to today is only slightly larger than predictions from stellar evolution (e.g., changes in the luminosity and color of the main-sequence turnoff and the morphology of the horizontal branch). A larger color difference is found in the red clusters, possibly suggesting that they are very metal-rich and/or significantly younger than 12 Gyr.

Subject headings: galaxies: elliptical and lenticular, cD – galaxies: star clusters – globular clusters: general – stars: evolution

1. INTRODUCTION

The formation of globular star clusters (GCs) is closely linked to the evolutionary histories of their parent galaxies. Major epochs of star formation in isolated galaxies as well as interactions with other galaxies lead to subsequent spikes in the number of GCs (Schweizer 1987; Ashman & Zepf 1998; Harris 2001; Brodie & Strader 2006). Indeed, it appears that the processes involved in galaxy formation imprint a signature on the clusters as reflected by the similar properties of the host galaxy and its associated clusters (e.g., age and metallicity). The prevalence of a large number of GCs around all massive galaxies, as well as their optically bright luminosities ($-10 \lesssim M_V \lesssim -5$), makes them excellent tracers of galaxy formation processes.

To date, GCs have been detected in hundreds of nearby

galaxies (see Table 1 in Brodie & Strader 2006 for those systems with accurate photometry). However, direct age measurements from resolved main-sequence turnoff fitting are only possible for the nearest clusters in the Milky Way, LMC, SMC, and M31 (e.g., see the recent study of SKHB 312 by Brown et al. 2004). Properties of more distant systems are typically constrained with integrated light photometry and, where possible, spectroscopy. Such work has demonstrated that the luminosity and color distributions of GCs in most galaxies are remarkably similar (e.g., Harris & Racine 1979), with most populations exhibiting a bimodal color distribution reflecting old metal-poor and metal-rich subpopulations. Whether these populations reflect GCs that formed at two different times (e.g., Forbes et al. 1997) is still debated. Unfortunately, directly probing the properties of these clusters at earlier times is a difficult task. For example, at the distance of the nearby Coma cluster, a typical GC with $M_V = -7.5$ has an apparent magnitude of $V = 27.5$.

In *HST* Cycle 13, our team (PI: Richer - GO-10424) was granted 126 orbits of ACS time in a single pointing to explore the white dwarf cooling sequence, faint main-sequence, and space motion of the Milky Way core-collapsed GC NGC 6397 (Richer et al. 2006; Hansen et al. 2007; Kalirai et al. 2007a). The resulting data set represents one of the deepest optical images ever obtained in astronomy, with a 50% (25%) completeness limit of $F814W = 28$ ($F814W = 28.75$) and a photometric error of $\sigma = 0.3$ at $F814W = 28.0$ and $F606W = 29.25$. In this *Letter*, we present the discovery of a distant, background galaxy in this data set that harbors its own GC population. We measure the redshift of the galaxy to be $z = 0.089$, and therefore this system resides ~ 375 Mpc from the Milky Way at a lookback

¹ Based on observations with the NASA/ESA Hubble Space Telescope, obtained at the Space Telescope Science Institute, which is operated by the Association of Universities for Research in Astronomy, Inc., under NASA contract NAS5-26555. These observations are associated with proposal GO-10424.

² Based on observations obtained at the Gemini Observatory, which is operated by the Association of Universities for Research in Astronomy, Inc., under a cooperative agreement with the NSF on behalf of the Gemini partnership: the National Science Foundation (United States), the Particle Physics and Astronomy Research Council (United Kingdom), the National Research Council (Canada), CONICYT (Chile), the Australian Research Council (Australia), CNPq (Brazil) and CONICET (Argentina).

³ University of California Observatories, University of California at Santa Cruz, Santa Cruz CA, 95060; jkalirai@ucolick.org

⁴ Harvard-Smithsonian Center for Astrophysics, Cambridge MA, 02138; jstrader@cfa.harvard.edu

⁵ Hubble Fellow

⁶ Space Telescope Science Institute, Baltimore MD, 21218; jayander@stsci.edu

⁷ Department of Physics and Astronomy, University of British Columbia, Vancouver, BC, Canada, V6T 1Z1; richer@astro.ubc.ca

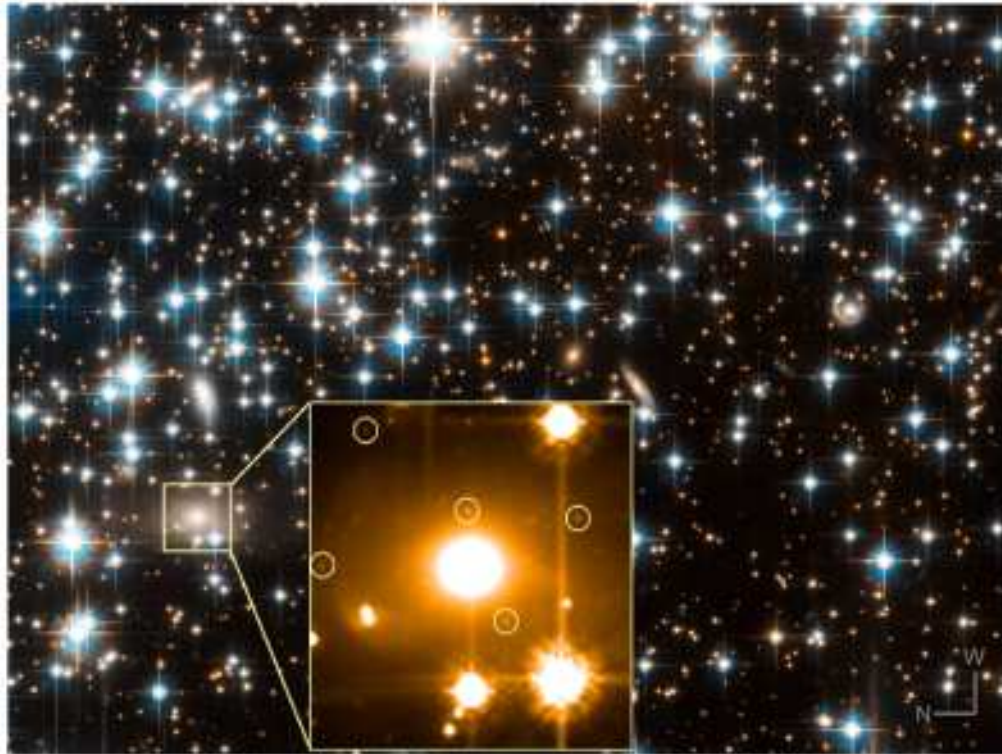


FIG. 1.— A $3.4' \times 1.7'$ section of the 126 orbit *HST* exposure of NGC 6397 (this is approximately one-half of the total ACS field of view). The strong gradient across the image from top-left to bottom-right reflects the decreasing radial density of NGC 6397 stars (the cluster center is located ~ 6.5 arcminutes to the N-W of our field). The inset shows a closer look ($8'' \times 8'' - 15.9 \times 15.9$ kpc at the distance of the elliptical galaxy) of the large elliptical galaxy at image coordinates $(x, y) = (789.9, 750.9)$ pixels. The point source enhancement surrounding the elliptical galaxy is very high and suggests that these objects are GCs themselves, orbiting this galaxy. Over the area of the inset, only one cluster white dwarf is expected to contaminate our sample. Five of the GCs are highlighted with small circles in the inset. Higher resolution version of this figure is available at <http://www.ucolick.org/~jkalirai/DistantGlobs/>. Image credit: NASA, ESA, H. Richer (UBC), J. Kalirai (UCSC).

time of 1.2 Gyr. The color function of the GCs in this galaxy is found to show differences when compared to local samples suggesting the possible detection of evolutionary changes in GC properties over the past Gyr.

2. IMAGING AND SPECTROSCOPIC OBSERVATIONS

The *HST*/ACS imaging observations of NGC 6397 from GO-10424 have been described in several papers (e.g., Richer et al. 2006; Hansen et al. 2007; Kalirai et al. 2007a; Anderson et al. 2008). To summarize, we obtained 252 images in *F814W* and 126 in *F606W*, for a total integration time of 126 orbits in a single pointing centered at $\alpha_{J2000} = 17:41:03$, $\delta_{J2000} = -53:44:21$. Sources detected at the same position on 90 of the 252 *F814W* images were shown to be a 3σ detection (from simulations) and cleaned to remove false detections in the wings of bright stars, those caused by intersecting diffraction spikes, and objects morphologically inconsistent with stars (e.g., galaxies and cosmic rays). PSF photometry on these sources was performed as described in Anderson et al. (2008).

Our expectation was that the final cleaned catalog of ~ 8000 objects from this analysis represented stars on the image. However, a spatial plot of the faint-blue sources indicated a clustering of 244 objects centered on a bright *F814W* = 16.7 elliptical galaxy at pixel location $x = 789.9$, $y = 750.9$ (see Figure 1). We reduced the ini-

tial catalogue by 6 objects that look extended, another 5 objects that are very bright and red, and 38 objects that were only detected in one filter and therefore for which we have no color information. This final sample of 195 objects must be GCs themselves, in orbit around the background galaxy. The clusters are among the faintest objects in our catalogue, ranging in brightness from $26 \lesssim F814W \lesssim 30$. Given the ACS pixel scale and distance to the galaxy (see below), these clusters are all located within a radial distance of $1.7 - 20$ kpc ($0.85'' - 10''$) from the center of this galaxy. The incompleteness in our sample increases rapidly as we approach the center of the galaxy and therefore we preferentially detect the bluer clusters. We can roughly estimate the masses of the clusters assuming they are old (12 Gyr) and metal-poor ($[\text{Fe}/\text{H}] = -1.5$). For a Kroupa initial-mass function, the Maraston (2005) models indicate that the GCs with *F814W* = 27.5 are $\sim 2 \times 10^6 M_{\odot}$ whereas the brightest globulars in this galaxy are $\sim 10^7 M_{\odot}$.

To measure the distance to the galaxy accurately, we first obtained a ground based image of the field in excellent seeing conditions and low air-mass with the Gemini Multi-Object Spectrograph (GMOS) on Gemini South (Program ID: GS-2006A-DD-16, executed on 18 Aug. 2006). Despite the confusion from NGC 6397 stars, the elliptical galaxy was easily delineated at $\alpha_{J2000} = 17:41:12.2$, $\delta_{J2000} = -53:43:16.5$ in a 120 s exposure with

the g' filter. Next, we obtained a low resolution spectrum of the galaxy with a $1''$ longslit and the B600 grating ($R = 1600$) centered at 5200 \AA . The position angle was set to 325 degrees to avoid contamination in the slit from nearby stars. Four 900 s target exposures, as well as observations of a flux standard, a Cu/Ar arc, and a flat field were obtained. The data were reduced using the Gemini IRAF Package, Version 1.8.

The final reduced spectrum of the elliptical galaxy in the observed wavelength frame of reference is shown in Figure 2 (top). The arrows mark several well-defined spectral features along with their rest-frame wavelengths. A cross-correlation with a template spectrum of an old, metal-rich single stellar population yields a best-fit redshift of $z = 0.0894$. Assuming standard concordance cosmology with $\Omega_m = 0.3$, $\Omega_\Lambda = 0.7$, and $h = 0.7$, this redshift corresponds to a proper radial distance of 375 Mpc and a lookback time of 1.2 Gyr . The luminosity distance of 409 Mpc gives a distance modulus of $m - M = 38.06$. While this is not the most distant galaxy in which GCs have been detected (that currently belongs to Abell 1689 at $z = 0.183$; Mieske et al. 2004), the photometry in this galaxy is considerably deeper than in any previous study of a galaxy at a comparable distance.

3. RESULTS – PHOTOMETRIC PROPERTIES OF DISTANT GLOBULAR CLUSTERS

To probe the properties of these distant GCs, we compare their color distribution to that of globulars in local elliptical galaxies. These galaxies nearly always have a bimodal distribution of GC colors, with peaks near $V - I \sim 0.95$ and 1.18 . There is a mild dependence of the peak GC colors with host galaxy luminosity (Strader, Brodie, & Forbes 2004; Peng et al. 2006), and so we correct these values to $V - I \sim 0.93$ and 1.16 for a galaxy with $M_V = -20.5$ (assuming $V - I = 1.2$). We note that our measurement of the integrated brightness of the galaxy is only roughly correct given the large number of foreground contaminating stars in the outer parts. This does not effect our results as a 0.5 magnitude difference in the galaxy luminosity would translate to a <0.01 mean magnitude offset in the expected peak color of the GCs.

In Figure 2 (middle) we present the color magnitude diagram of 196 GCs . This includes the foreground globular NGC 6397 where we resolve all of the individual stars (*small points*) as well as the 195 extragalactic objects (*larger points below the white dwarf cooling sequence of NGC 6397*). A large fraction of these distant GCs ($\sim 60\%$) have very faint magnitudes and lie below the 50% completeness limit (*dashed line, $F814W = 28$*). A total of 46 objects, or ~ 64 after accounting for incompleteness, have $F814W < 27.5$. The foreground reddening in the direction of NGC 6397 is $E(F606W - F814W) = 0.18$ (Hansen et al. 2007), giving $A_{F814W} = 0.33$ for a standard reddening curve. Using the distance modulus in §2 and this reddening, the expected peak of the approximately lognormal GC luminosity function (GCLF) is at $F814W \sim 30.0$. It follows that we have only observed the tip of the GCLF in this galaxy. Assuming a standard $\sigma = 1.3$ for the GCLF (e.g., Kundu & Whitmore 2001), down to $F814W = 27.5$ only $\sim 2.7\%$ of the total GC population is visible (assuming a Gaussian form for the entire GCLF). Even though this estimate is very

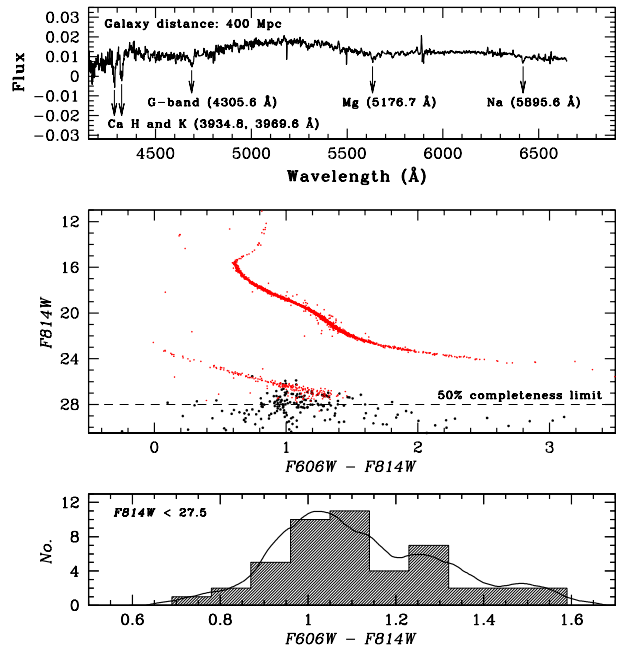


FIG. 2.— *Top* – A Gemini GMOS spectrum of the elliptical galaxy shown in Figure 1 reveals its redshift to be $z = 0.0894$, indicating a luminosity distance of 409 Mpc . Several absorption features and their rest-frame wavelengths are illustrated. *Middle* – The proper motion selected color-magnitude diagram of the foreground cluster NGC 6397 shows a beautiful main-sequence extending from the turnoff down to the lowest mass stars that burn hydrogen (red points). The rich white dwarf cooling sequence of the cluster is also visible. The larger dots in the faint-blue part of the CMD represent the 195 extragalactic GCs found in the vicinity of the large elliptical galaxy in Figure 1. *Bottom* – Histogram and density estimate for the colors of 46 GCs with $F814W < 27.5$. The majority of GCs belong to the blue subpopulation, with a tail towards red objects.

rough, it appears that there must be more than a thousand GCs in this galaxy. This puts the galaxy squarely in the regime of massive ellipticals, and we can safely use the peak GC colors of local ellipticals as a reference.

In Figure 2 (bottom) we show a color histogram of GC candidates with $F814W < 27.5$ and a density estimate overplotted. There is a broad peak of blue objects with $F606W - F814W$ between ~ 0.8 and 1.2 , and a tail to redder values. Mixture modeling of the color distribution with Nmix (see discussion in Strader et al. 2006) finds that the preferred fit is two Gaussians centered at $F606W - F814W = 1.03 \pm 0.02$ and 1.29 ± 0.05 . The errors are derived through bootstrapping. While increasing photometric errors tend to broaden the color distribution as one goes to fainter magnitudes, performing the same fitting to a limit of $F814W = 28$ yields essentially the same result: a preference for two populations of GCs, with peaks at $F606W - F814W = 1.03$ and 1.31 . The small number of red GCs makes that peak value uncertain, but the derived blue peak appears consistent with a visual estimate from Figure 2 (bottom).

We now compare these observed peak values to those expected from a scaling of local GC systems in a galaxy with same luminosity as our host elliptical. To convert from $V - I$ to $F606W - F814W$, we use the empirical relation of Harris et al. (2007), derived from photometry of NGC 2419. This relation is $F606W - F814W = 0.707(V - I) + 0.033(V - I)^2$. To these values we add

Galactic reddening of $E(F606W - F814W) = 0.18 \pm 0.03$. Finally, we add a k -correction derived from Bruzual & Charlot (2003) stellar population models. This depends slightly on the (unknown) metallicity of the stellar population, but assuming values of $[Fe/H] \sim -1.2$ and -0.2 for the two subpopulations gives k -corrections of 0.088 and 0.063, respectively. If our assumed metallicities are incorrect, the effect on the $F606W - F814W$ colors is minor: a 0.1 dex change in $[Fe/H]$ corresponds to about 0.01 mag, and 0.2 dex is a reasonable assumption for the uncertainty in the metallicity. Combining these corrections together gives predicted peak values of $F606W - F814W = 0.95 \pm 0.03$ and 1.11 ± 0.04 *disregarding* evolution in the stellar population. We also computed the predicted peak colors assuming the Sirianni et al. (2005) transformations between Vega magnitudes and ACS filters and found the same results, within the small error bars.

The observed change in the peak colors of blue and red GCs from $z = 0.089$ to today is 0.08 ± 0.04 and 0.18 ± 0.06 magnitudes. What is the expected evolution? Both the Maraston (2005) and Bruzual & Charlot (2003) models predict that the red metal-rich GCs should be about 0.01 mag redder in $F606W - F814W$ at the present day, and that there should be essentially *no* (< 0.01 mag) evolution in the blue metal-poor GCs. Therefore, to first order, our results suggest that more evolution has occurred than is predicted by the models, especially for the red clusters⁸. We note that some GC systems in the local universe show the peculiar property of a correlation between blue GC magnitude and color, such that the more luminous GCs are redder (Harris et al. 2006; Strader et al. 2006; Mieske et al. 2006). Since we sample only the brightest GCs in this distant galaxy, the mean color of the blue GCs derived above may be redder than the typical object, therefore bringing the predicted and observed values closer to the expected difference. We therefore conclude that the behavior of the blue GCs is essentially consistent with simple stellar population models, while the red GCs are substantially redder at a lookback time of ~ 1.2 Gyr than expected.

4. DISCUSSION

The most obvious candidate for any change in blue GC colors is the horizontal branch (HB). At old ages, its morphology is highly sensitive to a number of variables, including age. At younger ages, GCs should typically have red HBs, which transition to blue HBs as the stellar population ages. For old systems, the quantitative evolution in a relatively red color such as $F606W - F814W$ is expected to be small. Our results confirm this, suggesting that blue GCs have become bluer by just 0.08 ± 0.04 magnitudes over the past 1.2 Gyr. The Maraston (2005) models for a 12–13 Gyr metal-poor ($[Z/H] = -1.35$) single stellar population predict a difference of only 0.02 mag between an object with a blue and a red HB, consistent with our result at 1.5σ . Observations of Galactic GCs show no correlation between residuals of $V - I$ colors from a fiducial $V - I$ to $[Fe/H]$ relation and two different parameterizations of HB morphology, suggesting that—at least for the range of HBs observed in the Galaxy—the

HB has little effect on the $V - I$ color (Smith & Strader 2007).

For the red GCs, our mixture modeling fit of the color distribution indicates a peak at $F606W - F814W = 1.29 \pm 0.05$, 0.18 ± 0.06 magnitudes redder than the local sample. Although our data set contains few red GCs, the observed peak is found to be at the same color irrespective of the magnitude limit adopted (i.e., pushing the sample to $F814W < 28$). Over the past 1.2 Gyr, the expected evolution from models of a single stellar population is much smaller than this, as noted above. One possible way to reconcile *some* of these observed differences is to consider whether a fraction of these clusters are significantly younger than 12 Gyr, and more metal-rich. In this case, the predicted color difference resulting from standard stellar evolution between a redshift of $z = 0.089$ and now would be larger than that calculated above.

An additional effect may explain the observed color difference if the metallicities of the clusters are in fact supersolar. Recently, Kalirai et al. (2007b) have shown that the remnant population of white dwarfs in the old (8 Gyr), supersolar metallicity Galactic star cluster NGC 6791 are undermassive when compared to more metal-poor systems. These stars likely formed through a unique channel involving enhanced mass loss of the progenitor star on the red giant branch. Such evolution naturally explains both the absence of stars near the tip of the red giant branch in this cluster and the population of the extreme horizontal branch of the system (see also Castellani & Castellani 1993). Although the morphology of the horizontal branch does not heavily affect the color evolution of a population in our filters, the depletion of stars near the tip of the red giant branch can be more important and lead to an increasingly bluer population as the system ages. Of course, this mechanism would be even more efficient if the clusters are older since the envelope mass of the evolving stars is lower. However, this mechanism does require the clusters to have $[Fe/H] \gtrsim +0.2$ (Kilic, Stanek, & Pinsonneault 2007), and we see few systems nearby that are this metal-rich.

Finally, we note that these objects are far enough away that we cannot rule out a contaminating population of ultra-compact dwarfs (UCDs). The properties of these potentially transition objects (between GCs and dwarf galaxies) vary widely among galaxies. For example, in NGC 3311, they are seen as very red objects more luminous than the old and red GC population (Wegner & Harris 2007). However, in NGC 1407, the UCDs have larger sizes than globulars but have colors that fall between the blue and red subpopulations (Harris et al. 2006). We note that UCDs are typically found in massive galaxy clusters or “groups”, and it is difficult to assess the environment near our elliptical galaxy given the presence of NGC 6397 stars out to several arcminutes ($1' = 120$ kpc).

5. CONCLUSIONS

We have presented a study of the photometric properties of one of the most distant sample of GCs yet discovered, 195 objects at $d = 400$ Mpc. These clusters are all found around a bright elliptical galaxy that is itself located behind one of the nearest Galactic GCs to the Sun, NGC 6397. Given their large distance, the light

⁸ Based on the tightness of NGC 6397’s main-sequence, the differential reddening along this line of sight is negligible.

from these clusters has taken 1.2 Gyr to reach us, and therefore these objects offer us a rare chance to probe the evolution of GCs in the recent past. By comparing the color function of these clusters to nearby GCs, we find differences that suggest the mean colors of GCs have become bluer in the past Gyr. This evolutionary change can be explained assuming standard stellar evolution for the blue clusters. However, we find differences that suggest the mean colors of the red GCs were significantly redder 1.2 Gyr ago as compared to samples in local giant ellipticals, much redder than evolutionary models predict.

We would like to thank the entire *HST*/ACS team from GO-10424 for their help in obtaining the imaging observations. We are also grateful to the Gemini South obser-

vatory for approving our program under the Director's Discretionary Time allotment (Program ID: GS-2006A-DD-16). We would also like to thank an anonymous referee for several useful suggestions that have improved the quality of this Letter, and for his/her patience through the refereeing process. JSK and JS are both supported by NASA through Hubble Fellowship grants, awarded by the Space Telescope Science Institute, which is operated by the Association of Universities for Research in Astronomy, Incorporated, under NASA contract NAS5-26555. Support for this work was also provided by grant HST-GO-10424 from NASA/STScI. The research of HBR is supported by grants from the Natural Sciences and Engineering Research Council of Canada. He also thanks the Canada-US Fulbright Program for the award of a Fulbright Fellowship.

REFERENCES

- Anderson, J., et al. 2008, *AJ*, 135, 2114
 Ashman, K. M., & Zepf, S. E. 1998, *Globular Cluster Systems*, Cambridge, U. K.; New York : Cambridge University Press, 1998
 Brodie, J. P., & Strader, J. 2006, *ARA&A*, 44, 193
 Brown, T. M., Ferguson, H. C., Smith, E., Kimble, R. A., Sweigart, A. V., Renzini, A., Rich, R. M., & VandenBerg, D. A. 2004, *ApJ*, 613, L125
 Bruzual, G., & Charlot, S. 2003, *MNRAS*, 344, 1000
 Castellani, M., & Castellani, V. 1993, *ApJ*, 407, 649
 Forbes, D. A., Brodie, J. P., & Grillmair, C. J. 1997, *AJ*, 113, 1652
 Hansen, B. M. S., et al. 2007, *ApJ*, 671, 380
 Harris, W. E., & Racine, R. 1979, *ARA&A*, 17, 241
 Harris, W. E. 2001, *Extragalactic Star Clusters*, IAU Symposium 207, ed. E. Grebel, D. Geisler, D. Minniti, astro-ph/0108355
 Harris, W. E., Whitmore, B. C., Karakla, D., Okon, W., Baum, W. A., Hanes, D. A., & Kavelaars, J. J. 2006, *ApJ*, 636, 90
 Harris, W. E., Harris, G. L. H., Layden, A. C., & Stetson, P. B. 2007, *AJ*, 134, 43
 Kalirai, J. S., et al. 2007a, *ApJ*, 657, L93
 Kalirai, J. S., Bergeron, P., Hansen, B. M. S., Kelson, D. D., Reitzel, D. B., Rich, R. M., & Richer, H. B. 2007b, *ApJ*, 671, 748
 Kilic, M., Stanek, K. Z., & Pinsonneault, M. H. 2007, *ApJ*, 671, 761
 Kundu, A., & Whitmore, B. C. 2001, *AJ*, 121, 2950
 Maraston, C. 2005, *MNRAS*, 362, 799
 Mieske, S., et al. 2004, *AJ*, 128, 1529
 Mieske, S., Hilker, M., Infante, L., & Jordan, A. 2006, *AJ*, 131, 2442
 Peng, E. W., et al. 2006, *ApJ*, 639, 95
 Richer, H. B., et al. 2006, *Science*, 313, 936
 Schweizer, F. 1987, *Philos. Trans. R. Soc. London Ser. A* 358, 2063
 Sirianni, M., et al. 2005, *PASP*, 117, 1049
 Smith, G. H., & Strader, J. 2007, *Astronomische Nachrichten*, 328, 107
 Strader, J., Brodie, J. P., Forbes, D. A., 2004, *AJ*, 127, 3431
 Strader, J., Brodie, J. P., Spitler, L., & Beasley, M. 2006, *AJ*, 132, 2333
 Wehner, E. M. H., & Harris, W. E. 2007, *ApJ*, 668, L35